Construction of a Lithium Photoassociation Laser

Ryne T. Saxe
The University of Alabama, Tuscaloosa, AL

Since the advent of laser cooling and the demonstration of Bose-Einstein condensation, physicists have refined experimental techniques to study specific atomic transitions and manipulate atomic interactions, resulting in the production of new types of molecules. Photoassociation is one such technique. This paper discusses the construction of a Lithium photoassociation laser system for the production of diatomic LiYb. Results of initial diagnostic testing are presented and discussed.

I. Introduction

Much of experimental atomic physics involves the interaction of matter with light, often utilizing laser systems that may be tuned to atomic resonance transitions. In particular, advanced techniques such as laser cooling and optical trapping have thrust this field into a new era. These methods give physicists the ability to control atomic and molecular interactions at ultra-cold temperatures, within certain degrees of freedom. Under these conditions, physicists can perform spectroscopy with unparalleled resolution, study exotic states of matter and even synthesize new types of molecules.

A. What is Photoassociation?

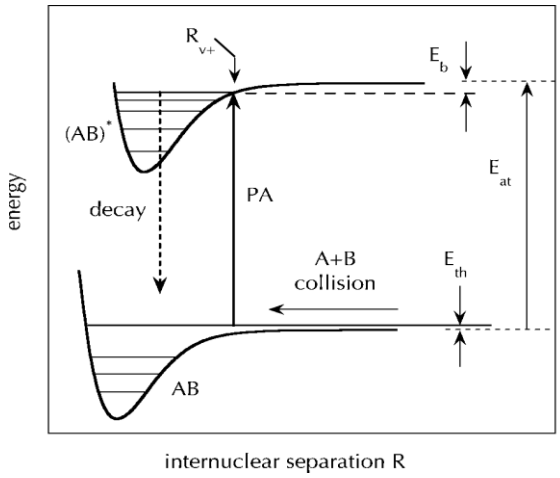

Figure 1. Schematic illustrating Equation 1. [1]

When a trapped gas of atoms is illuminated with light at just the right frequency, two colliding atoms may absorb a photon and *photoassociate* to form a bound molecule in an electronically excited state [1]:

$$A + B + \gamma \rightarrow (AB)^* \qquad (1)$$

Typically, the excited molecule quickly decays; the final product of this decay can be either two free atoms of a bound, ground state molecule:

$$(AB)^* \rightarrow A + B + \gamma_{decay} \quad or \quad (AB)^* \rightarrow AB + \gamma_{decay} \qquad (2)$$

By precisely controlling the frequency of the light source, physicists may employ photoassociation techniques to produce ultra-cold molecules and resolve their exact binding energies (and, in turn, determine scattering length).

B. Photoassociation Spectroscopy

Development of laser cooling techniques allows photoassociation (hereafter PA) spectroscopy to be performed at very high resolution. By this method, physicists may resolve and map molecular energy levels and investigate molecules whose properties are closely related to the properties of their constituent atoms.

In order to achieve a sufficient PA rate for spectroscopy (i.e. to produce enough molecules to obtain an energy spectrum), there are several experimental conditions which must be accounted for. Initially, sample atoms should be slowed, trapped and confined within the cross-section of the light beam used to initiate PA transitions. To achieve this, atoms may initially be slowed and cooled into an 'optical molasses' state through a Zeeman slower, and then confined under vacuum within a magneto-optical trap (MOT). To maximize PA rate, trapped atoms should be held under ultra-cold ($\leq$ 1mK) conditions so that their kinetic energy spread is on the

order of (or less than) the natural linewidth of an excited molecular state [1]. The light which drives the PA process is then typically supplied independently by a narrow-linewidth laser system that is tunable over a range of frequencies corresponding to excited molecular rovibrational energy levels. This description provides a most basic overview of the setup employed in our own laboratory.

Most simply, a PA spectrum measures the number of excited molecules produced as a function of the frequency of the applied light [1]. For *one-photon* PA experiments seeking to resolve electronically excited molecules, spectra are recorded by monitoring the number of atoms lost from the MOT. As the source laser beam is directed and tuned through the trapped atom cloud, newly formed diatomic molecules decay as noted in the Section IA. Both signature PA decay processes induce *trap loss*: a) if the excited molecule decays back into two atoms, these atoms carry enough momentum to escape the MOT, *or* b) if the molecule decays into a bound ground state, it is no longer in resonance with the trap beams and will escape. Trap loss can be detected by monitoring the fluorescence of the trapped atom cloud; as the PA laser is scanned over a range of frequencies, one will observe a loss of intensity at frequencies corresponding to PA transitions into excited molecular energy levels; an example spectrum is shown in Figure 2, where the x-axis represents arbitrary units of displacement from some known atomic transition line. By using a source laser that features a narrow linewidth over its range of tunability, one can resolve individual states to a high level of accuracy.

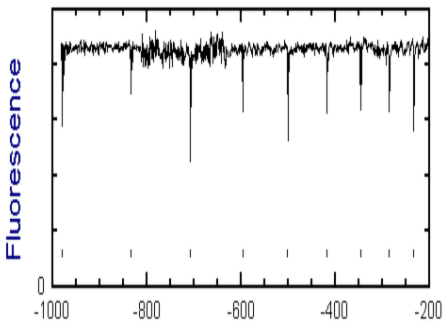

Figure 2. [2]

As an additional note, *two-photon* PA experiments may be performed to investigate *ground-state* energy levels of the molecule produced. By this method, an additional laser is employed to drive transitions between an excited energy state and the ground state of interest. After molecules are initially produced, the frequency of this second laser is tuned over the bound-bound transition range. As this laser is tuned into resonance, it perturbs excited molecules to fall to the ground state, and *reduces* the rate of trap loss induced by initial PA processes. It follows that ground-state PA spectroscopy may be performed by monitoring the subsequent *increase* in trap fluorescence.

II. Lithium Photoassociation Laser

A diode laser system proves to be a good candidate for driving PA transitions. Diode lasers have improved remarkably and are readily available and affordable. Most importantly, a diode laser system can offer narrow-bandwidth, frequency-stabilized operation and can be assembled to tune over an adequate frequency range to resolve different molecular energy states.

In our experiments, we seek to drive PA resonant transitions occurring just below the D2 atomic energy levels for Lithium, which is known to occur at 670.971nm (energy level diagram shown in Appendix). Our PA laser must scan over a range of wavelengths that are 'red-detuned' from this transition, which serves as an asymptotic value for bound excited Lithium molecules (recall Figure 1 for general illustration). Red laser diodes optimized for operation at 670-671nm are widely available. For our system, we selected a ridge waveguide laser diode from Eagleyard Photonics centered at 670nm. The ridge waveguide configuration improves tunability and gain feedback and increases power output.

Controlling optical feedback was the primary concern for determining how to physically mount the laser diode. Our system features an extended-cavity assembly designed to provide frequency-selective feedback to the diode in order to achieve narrow linewidth and maximize stable tunability. An extended-cavity diode laser (ECDL) may be constructed using relatively few components and integrated into a compact assembly.

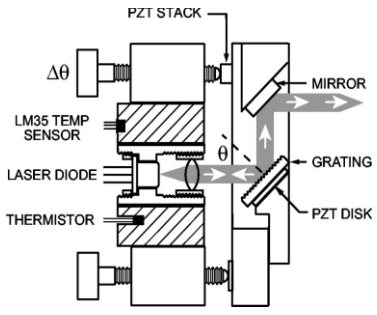

Figure 3. [4]

The essential requirement for an ECDL is that the diode, diffraction grating (which provides the necessary feedback) and collimating optics all be mounted rigidly with respect to each other, and that the angle of the grating and position of the lens be precisely adjustable [3]. These requirements may be satisfied by integrating commercial components, with a few slight modifications. To achieve frequency-selective feedback to the diode, output optics were mounted in common Littrow configuration. In this configuration, the diode output is collimated using a simple aspheric lens – both mounted in a lens tube – and the first-order diffraction from a grating is coupled back into the laser diode to provide optical feedback; at this 'seed point' the reflected light interferes to form the laser output beam.

For our general design for mounting the laser diode, we refer to the method of Arnold, Wilson, and Boshier [3] with modifications applied by Hawthorn, Weber and Scholten [4], as shown in Fig. 3. For simplicity, we made one slight alteration to the Hawthorn design by machining the grating/mirror mount in two separate pieces (Fig. 4a), secured to each other using two 4-40 screws.

In addition, we mounted the ECDL assembly over an aluminum base plate connected to a thermo-electric controller, which received feedback from an integrated thermocouple to control temperature stability. This simple planar conductive heating mechanism ensures that the ECDL is heated evenly. The ECDL mirror mount may be secured to the base plate using an adhesive, or may be screwed down after machining an additional counter-bored thru-hole in the bottom of the mirror mount. For clarification, refer to Figures 4b. Finally, the ECDL assembly was mounted over stacked rubber and brass base pieces for mechanical isolation. The entire assembly is housed in an acrylic chassis – about the size of a shoebox – that is lined with acoustic isolation material and features all necessary electrical connections, as shown in final photograph (Fig. 4c).

---

a) 

b) 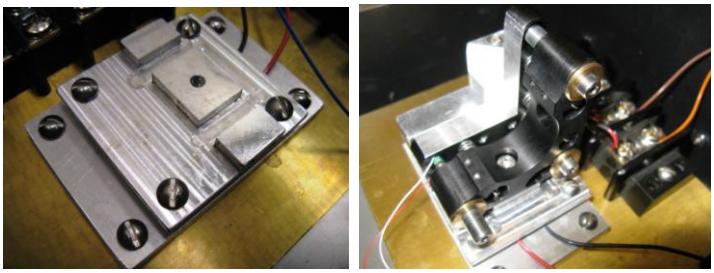

c) 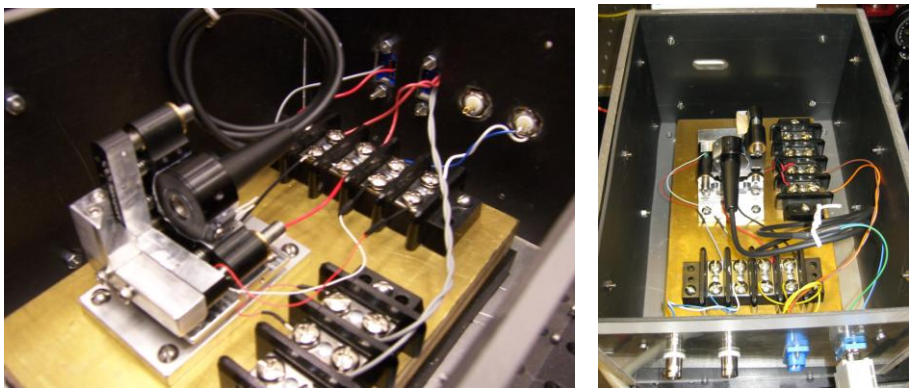

Figure 4. *Figure 4a shows the modification made to the Hawthorn grating mount design. Figure 4b shows the aluminum base piece and assembled mirror/grating mount secured to base. Figure 4c shows assembly in box with collimation tube mounted.*

III. Alignment & Testing

With the laser diode properly mounted and the ECDL assembly in place, initial tests were carried out to study performance parameters and characterize the laser's tunability. At first, only a current controller (ThorLabs LDC Series) was connected to ensure that the diode would light up; the temperature circuit was left open, as temperature variability is not important for initial alignment and power measurements. The beam was collimated by adjusting the aspherical lens position in the lens tube holding the diode. The first

basic test is to map diode output power versus diode current, and to compare this curve with the one supplied by the diode manufacturer.

Next the diffraction grating angle was adjusted (via the mirror mount) in order to align the first-order diffraction mode back into the diode. This was done by tracing the mode's reflection on a white card as the grating angle was adjusted. At the point where this reflection coincides with the collimated beam spot, the diode recognizes optical feedback and begins to lase at lower current threshold and narrow linewidth. This 'seed point' is accompanied by a noticeable spike in beam intensity and output power (monitored with Thorlabs power meter). This spike is most apparent if this initial alignment procedure is carried out with the diode current set just below its 'threshold current' for laser operation, as given in manufacturer documentation. For our diode, this point was specified to occur around 75mA; the alignment procedure was done at 68mA. Once seeded, the threshold current value for the laser diode should decrease slightly. At this point, the laser beam was focused through an external optical isolator to protect against unwanted, back-reflected optical feedback that could interfere with laser stability or even damage the diode. With the critical optics properly aligned and the diode receiving feedback, one can proceed to test performance parameters.

To understand the characteristics of this particular laser diode, we investigated its response to variable current and temperature in terms of output power and wavelength. The test of output power versus diode current was repeated for seeded laser power, to be compared with the curve initially obtained for the unseeded diode. In addition, we tested the laser diode's response to temperature, plotted as wavelength vs. temperature. In these tests, we were particularly interested in the extreme wavelength values, which bound the range of tunability. We were also interested in how these bounds shifted higher as diode temperature increased. For each round of temperature testing, power measurements were taken at each data point in order to track how output power levels and peak power points were affected by increasing diode temperature. Next, power values were plotted as a function of wavelength in order to trace the diode's output power curve; this curve clearly displays points of peak power output, as well as the diode behavior near wavelength bounds. Power curves were obtained for incremental diode temperatures. Finally, we swept the piezo circuit at variable frequency and voltage input in order to investigate laser response as a function of input voltage. In these tests, the laser was coupled into a Fabry-Perot etalon to display its mode behavior on an oscilloscope and track mode shifts while variable voltage drove the piezo to alter optical cavity length; this test can be quantified into a result in terms of [frequency response]/Voltage (MHz/V). All relevant plots and discussion from these initial tests rounds are presented in sequence below.

IV. Results & Discussion

Plots are displayed below that correspond to each round of testing. For tabulated data point values, refer to Appendix.

Graph A

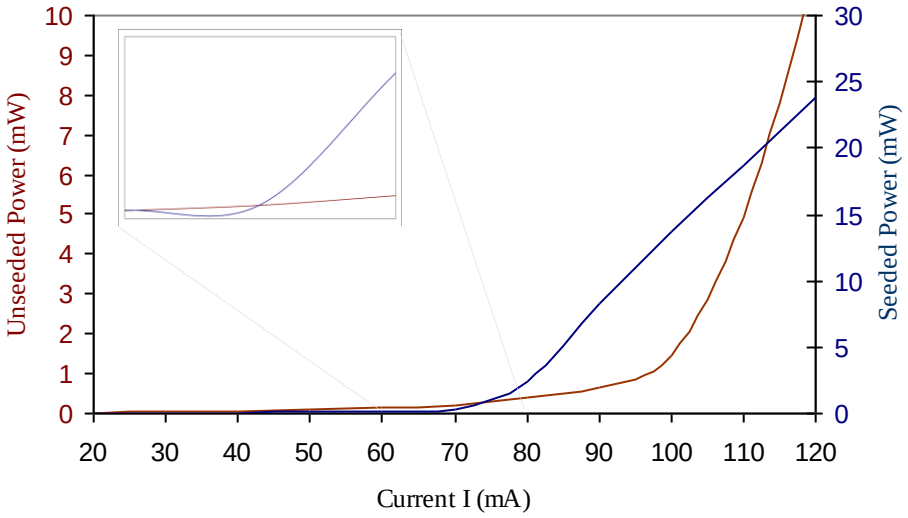

The above graph (Graph A) corresponds to initial tests taken to plot power versus diode current. For comparison, both 'unseeded' (crimson) and 'seeded' (blue) data series are included. It is easily recognizable that the seed point shifts the laser threshold to a lower current value, where the power rises abruptly in a linear trend. The unseeded threshold is more ambiguous, with power increasing in a non-linear trend; this curve closely matches the test curve provided by the manufacturer. The embedded graph displays a 'zoomed-in' view in the current range of 60-80mA, plotted according to a single power axis (y-axis).

Graph B

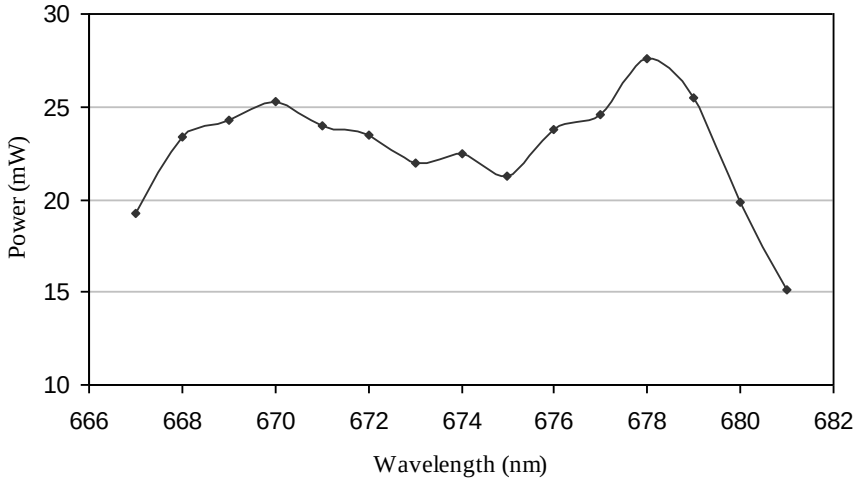

The above graph (B) shows the power curve over the entire tunable range (achieved through adjusting grating position) at 25°C. The curve tends to a plateau shape, featuring two maxima, rather than a Gaussian profile with a central maximum. This seems to be a characteristic of the particular diode, and this trend shape is fairly consistent at increased diode temperatures. See following graph (Graph C).

Graph C

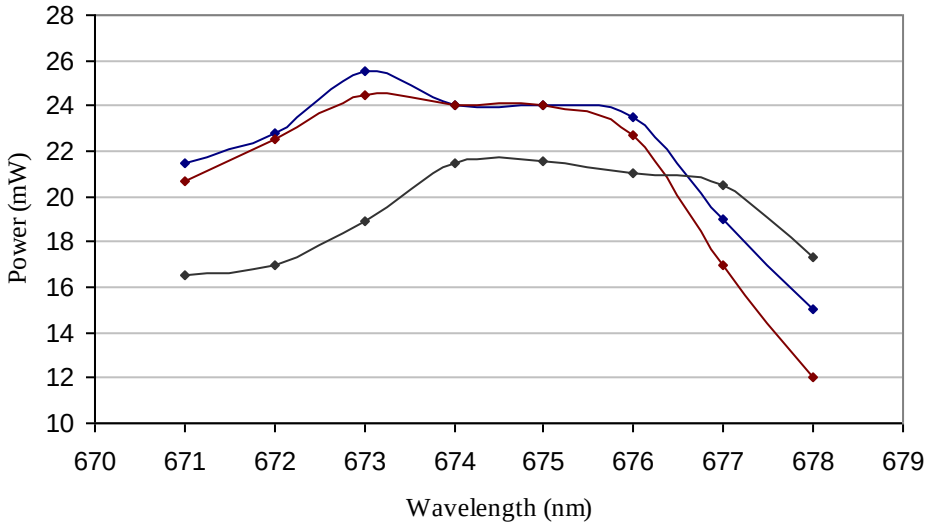

For comparison, the above graph (C) displays power curves over the central 50% of tunable wavelength range for three different diode temperatures: the blue curve corresponds to T=25°C; the crimson curve corresponds to T=30°C; the grey curve corresponds to T=35°C. Notice that the plateau shape remains consistent for each temperature series. As expected, average power values decrease for increasing temperature. Also, as expected, the increased temperature series at 35°C shows a shift in the curve to the right as higher wavelengths become accessible.

Graph D

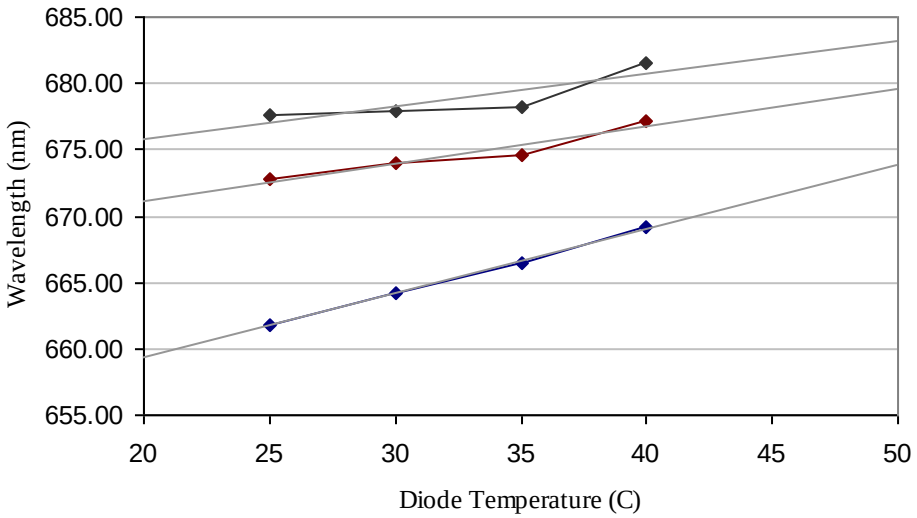

The final graph (D) plots wavelength versus increasing diode temperature. The blue data series corresponds to the lower wavelength bound of the tunable range, where the diode becomes 'unseeded' and absolute power drops below 12 mW. The crimson data series corresponds to the points of peak power in the tunable range. The grey data series corresponds to upper wavelength bounds of the tunable range. As expected, trends are nearly linear as temperature is increased; trend lines are plotted.

NOTES: Laser box was mounted on an optical breadboard for testing, with a mirror (Thorlabs EO2) placed at the beam exit hole to deflect beam (at a right angle) through a focusing lens and optical isolator (80% power through isolator). All power measurements presented in graphs were taken with sensor placed between the lens and isolator to avoid reflecting beam back into diode.

As shown, the diode laser was tunable over a wavelength range of up to 15nm. The lower wavelength bounds seemed to be limited by the response of the wavemeter, rather than diode performance. With more precise beam alignment (and therefore more power entering wavemeter), it may be possible to extend the range of tunability to 20nm by decreasing the lower bound. In one series of informal testing, the diode did prove to be tunable down to 661nm before losing feedback.

At higher wavelengths (~676-682nm), diode power was more stable when slowly 'backing up' to desired wavelength (i.e. 'backing off' grating by adjusting screw counter-clockwise) versus increasing wavelength to desired point.

While the ridge waveguide laser diode operates as higher power and is more tunable than the existing Lithium laser, it is also slightly less stable – there is some fluctuation in power output and temperature stability. These effects are most pronounced at diode temperatures of >30°C, where power readings often fluctuated over a range of ±1mW.

Due to initial difficulties in sweep circuit, there was not enough time to adequately test piezo response. In one round of testing, frequency response to piezo voltage was about 50 Hz/V. However, this number has not been checked by subsequent rounds of testing.

Appendix

The following tables display data points obtained in testing and used to plot graphs displayed in Results section. The letter label of each table presented corresponds to the graph with the same letter (Table A corresponds to Graph A, etc.)

Table A

Diode Current (mA)	Unseeded Power* (mW)	Seeded Power* (mW)
10	0.011	0.011
20	0.024	0.024
30	0.040	0.040
40	0.059	0.061
50	0.088	0.090
60	0.135	0.140
70	0.222	0.231
80	0.379	2.400
90	0.650	8.300
100	1.440	13.700
110	4.900	18.650
120	11.000	23.800

*Power values represent averages from three test rounds.

Table B

λ (nm)	Power (mW) @ T=25
667.0	19.2
668.0	23.4
669.0	24.3
670.0	25.3
671.0	24.0
672.0	23.5
673.0	22.0
674.0	22.5
675.0	21.3
676.0	23.8
677.0	24.6
678.0	27.6
679.0	25.5
680.0	19.8
681.0	15.1

Table C

λ (nm)	Power* (mW) @ T=25	mW* @ T=30	mW* @ T=35
671.0	21.5	20.7	16.5
672.0	22.8	22.5	17.0
673.0	25.5	24.5	18.9
674.0	24.0	24.0	21.5
675.0	24.0	24.0	21.6
676.0	23.5	22.7	21.0
677.0	19.0	17.0	20.5
678.0	15.0	12.0	17.3

*Power values represent averages from three test rounds.

Table D

Temperature °C	Min λ (nm)*	Peak Power λ (nm)*	Max λ (nm)*
25	661.85	672.80	677.60
30	664.20	673.97	677.90
35	666.40	674.65	678.25
40	669.10	677.20	681.60

*Wavelength values represent averages from two test rounds.

References

[1] K. M. Jones, E. Tiesinga, P. D. Lett, P. S. Julienne, *Reviews of Modern Physics* **78**, 483 (2006).

[2] Hulet Atom Cooling Group, Rice University.
http://atomcool.rice.edu/?Research:Archive:Photoassociation_Experiments

[3] A. S. Arnold, J. S. Wilson, M. G. Boshier, *Review of Scientific Instruments* **69**, 1236 (1998).

[4] C. J. Hawthorn, K. P. Weber, R. E. Scholten, *Review of Scientific Instruments* **72**, 4477 (2001)